Available online at www.sciencedirect.com

ScienceDirect

Procedia Structural Integrity 17 (2019) 177–182

Structural Integrity Procedia

www.elsevier.com/locate/procedia

ICSI 2019 The 3rd International Conference on Structural Integrity

Effect of pre-strain on cyclic plastic behaviour of 7050-T6 aluminium alloy

R. Branco[a]*, L.P. Borrego[b,a], J.D. Costa[a], F.V. Antunes[a]

[a]*CEMUC, Department of Mechanical Engineering, University of Coimbra, Rua Luís Reis Santos, 3030-788 Coimbra, Portugal*
[b]*Department of Mechanical Engineering, Coimbra Polytechnic - ISEC, Rua Pedro Nunes, Quinta da Nora, 3030-199 Coimbra, Portugal*

Abstract

This paper aims at studying the pre-strain effect on cyclic plastic behaviour of the 7050-T6 aluminium alloy. In order to meet this goal, different series of tests with various pre-strain histories are performed under fully-reversed strain-controlled conditions. In a second stage, fracture surfaces are examined by scanning electron microscopy to identify the main fracture damage micro-mechanisms associated with the pre-strain scenarios. Overall, the results show that higher tensile pre-strain levels lead to lower fatigue lives. This reduction of the fatigue life expectancy tends to increase for higher cyclic strain amplitudes.

Peer-review under responsibility of the ICSI 2019 organizers.

Keywords: Pre-strain; low-cycle fatigue; cyclic plastic behaviour; 7050-T6 aluminium alloy;

1. Introduction

High-strength 7xxx series aluminium alloys are widely used in aeronautical applications due to their superior features, in particular the excellent strength-to-weight ratio, high stress-corrosion cracking resistance, good fracture toughness, and low cost [1-2]. Among them, the 7050 aluminium alloy has been one of the most used in the manufacturing of aircraft structural parts. Manufacturing cycles and assembly processes in these value-added products are susceptible to induce considerable amounts of pre-strain. However, pre-strain histories are not usually considered

* Corresponding author. Tel.: +351-239-790-700; fax: +351-239-403-407.
E-mail address: ricardo.branco@dem.uc.pt

2452-3216 © 2019 The Authors. Published by Elsevier B.V.
Peer-review under responsibility of the ICSI 2019 organizers.
10.1016/j.prostr.2019.08.024

Nomenclature

CS	cyclic strain
CH	cyclic hardening
E	Young's modulus
N	number of cycles
N_f	number of cycles to failure
PS	pre-strain level
SEM	scanning electron microscopy
Δ	elongation
$\Delta\varepsilon$	strain range
$\Delta\varepsilon/2$	strain amplitude
$\Delta\sigma$	stress range
$\Delta\sigma/2$	stress amplitude
ε	strain
σ	stress
σ_{YS}	yield strength
σ_{UTS}	ultimate tensile strength
ν	Poisson's ratio

in fatigue design of such parts. Literature results have shown that cyclic softening or cyclic hardening behaviour is dependent on the pre-strain level [3]. On the other hand, detrimental or beneficial effects on fatigue behaviour have been associated with the material type, pre-strain history, and type of applied loading, among others [4-7]. Although the 7050-T6 aluminum has been deeply studied over the years, the effect of pre-strain on cyclic plastic behaviour remains unclear.

This paper aims, therefore, to study the pre-strain effect on cyclic plastic behaviour of 7050-T6 aluminium alloy. In order to meet this goal, different series of tests with various pre-strain levels are performed under fully-reversed strain-controlled conditions at various strain amplitudes. After the tests, fracture surfaces are examined by scanning electron microscopy to identify the main damage micro-mechanisms associated with the various pre-strain histories.

2. Experimental procedure

The material used in this research was the quaternary Al-Zn-Mg-Cu 7050 aluminium alloy in the T6 condition. Its main mechanical properties are summarised in Table 1. The specimen geometry, exhibited in Figure 1, consisted of a 15mm-long and an 8mm-diameter gauge section. Fatigue tests were conducted at room temperature, under fully-reversed ($R_\varepsilon = -1$) strain-controlled conditions, with a constant strain rate ($d\varepsilon/dt = 8\times10^{-3}$ s^{-1}) and sinusoidal waveforms.

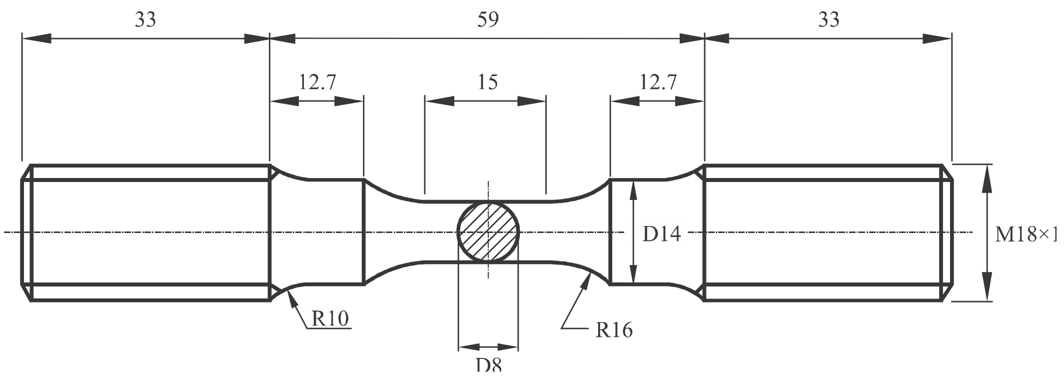

Fig. 1. Specimen geometry defined in accordance with the ASTM E606 standard.

Table 1. Monotonic mechanical properties of the 7050-T6 aluminum alloy.

σ_{YS} (MPa)	σ_{UTS} (MPa)	Δ (%)	E (GPa)	ν
546	621	14	71.7	0.33

Pre-strain (PS) was applied by monotonic tensile loading assuming three different levels, namely: 0% (i.e. no pre-strain), 4% and 8%. For each case, strain amplitudes ($\Delta\varepsilon/2$) varied in the range 0.6% to 1.5%. Stress-strain data were recorded using an electrical extensometer with a 12.5mm-long gauge clamped to the specimen via two separated knife-edges. After fatigue testing, fracture surfaces were examined by scanning electron microscopy.

3. Results and discussion

The typical cyclic stress-strain responses recorded in the strain-controlled low-cycle fatigue tests for the different monotonic tensile pre-strain histories are presented in Figure 2. This figure shows three tests performed at the same strain amplitude ($\Delta\varepsilon/2 = \pm 1.5\%$) with no pre-strain (PS=0%), 4% pre-strain (PS=4%), and 8% pre-strain (PS=8%). Pre-strain was applied by monotonic tensile loading until the prescribed pre-strain was reached. After that, loading was reduced to zero. Effective pre-strain values induced in the specimens were, respectively, 3.1% and 7.0% for the cases of PS=4% and PS=8% (see Figure 2). In the second stage of the tests, i.e. strain-controlled tests, fully-reversed conditions were assumed ($R_\varepsilon = -1$). The specimen diameter considered in the calculations corresponded to the values measured at the beginning of the second stage (i.e. after pre-straining). The differences in fatigue behaviour are assumed to be due to the pre-strain stage. As can be seen in Figure 2, irrespective of the pre-strain history, it can be clearly observed a cyclic strain-softening behaviour. Without pre-strain (PS=0%), tensile and compressive stresses vary in a soft manner during the test. On the contrary, as the pre-strain increases, the variations of both the tensile and the compressive stresses tend to be more relevant in each cycle and, therefore, along the test. This is evident by comparing the positions of the mid-life cycles of the three tests. The more intense changes at higher pre-strain values can be explained by the means stress relaxation behaviour. At lower pre-strain levels, relaxation phenomenon is more limited which results in higher mean stress levels (and, therefore, lower changes in peak stresses) during the entire

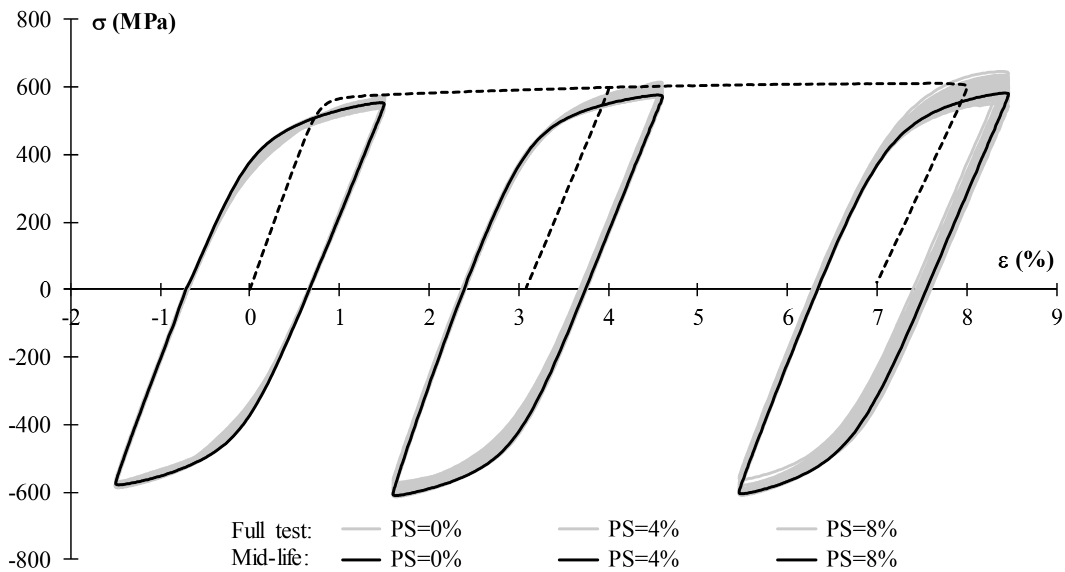

Fig. 2. Cyclic stress-strain response for various pre-strain levels.

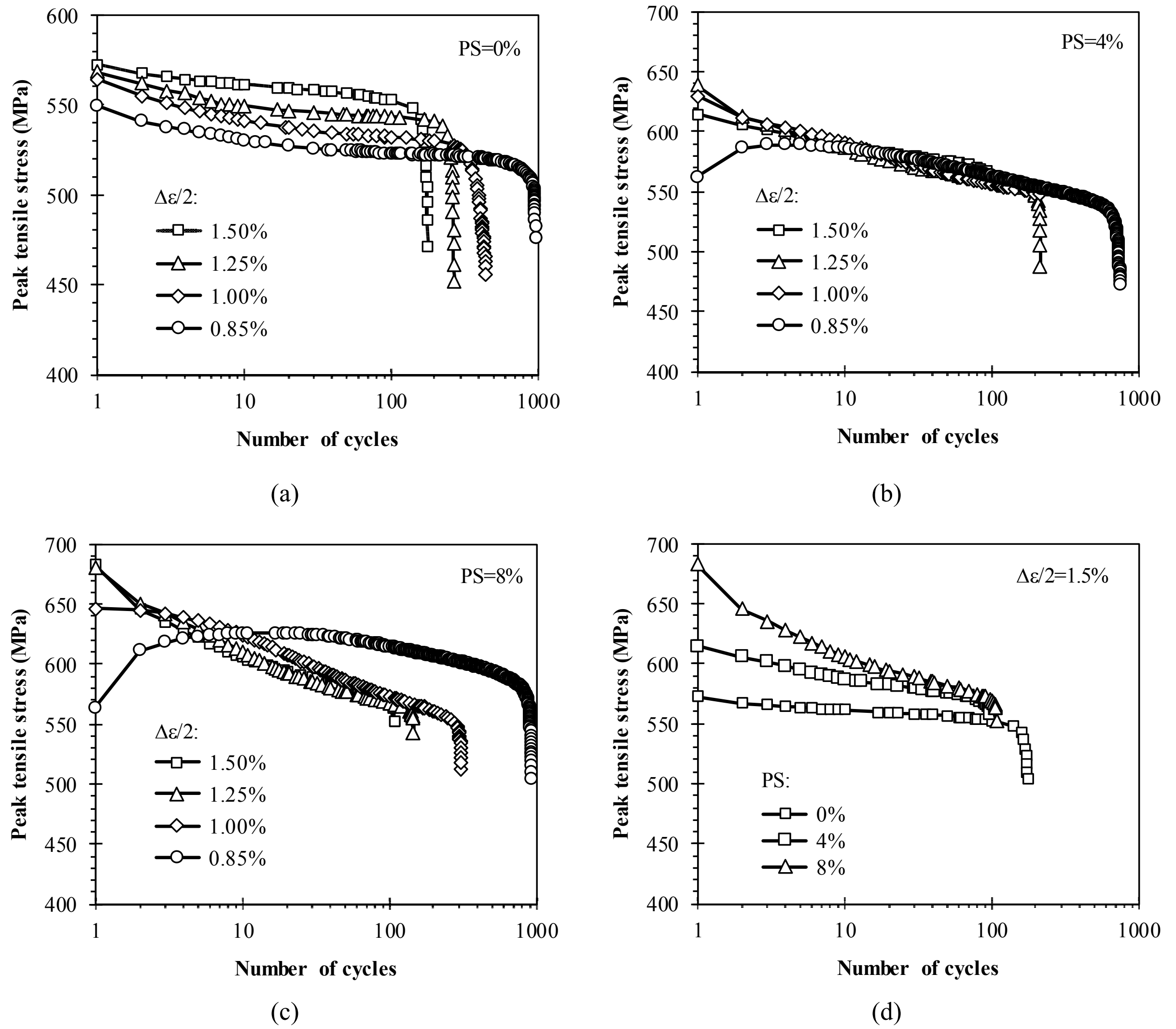

Fig. 3. Evolution of peak tensile stress: (a) with PS=0%, (b) with PS=4%, (c) with PS=8% at various strain amplitudes; (d) with Δε/2=1.5% and various pre-strain levels.

lifetime. In fact, as exhibited in Figure 5 which plots the peak tensile stresses against the number of cycles to failure, at PS=0%, the more relevant variations occur in the first few cycles, and all cases evidence a cyclic strain-softening behaviour. After that, peak tensile stresses tend to be similar and only at the final stage is observed a fast decay until failure occurs. Regarding the cases of PS=4%, it can be also observed an initial period of fast variations, but there is no a clear stabilised behaviour since the peak tensile stresses reduce progressively. At higher strain amplitudes, it can be identified a cyclic strain-softening behaviour while, at lower strain amplitudes, there is an initial increase of the peak tensile stress which is a sign of cyclic strain-hardening behaviour. With respect to the cases of PS=8%, the conclusions are similar to the latter case. There is a mixed cyclic softening-hardening behaviour which is dependent on the strain amplitude. Nevertheless, in this case, the decrease of the peak tensile stress is more intense. These variations can be explained by the higher mean stress relaxation phenomena resulting from the higher pre-strain levels induced in the specimens. The increase of the mean stress relaxation rates due to increasing pre-strain levels can be clearly distinguished in Figure 3(d). In the absence of pre-strain, peak tensile stresses suffer slight variations in the first cycles and then maintain an almost constant value until failure occurs. With pre-strain, peak tensile stresses converge to the peak tensile values of the case PS=0% (see Figure 3(d)).

The relationship between the total strain amplitude and the number of reversals to failure for different pre-strain levels is plotted in Figure 4. Although there are some exceptions, fatigue life reduces with increasing pre-strain histories. In general, the differences tend to be more relevant at higher strain amplitudes while, at lower strain amplitudes, the relative differences are attenuated. For the sake of clarity, only the fitted functions of the low-cycle fatigue results for the tests with no pre-strain (i.e. PS=0%) are presented.

Figure 5 shows two micrographies obtained at high magnification (2000x) in samples subjected to similar pre-strain (PS=8%) and different strain amplitude ($\Delta\varepsilon/2 = 1.5\%$, and $\Delta\varepsilon/2 = 0.6\%$). The main features associated with the

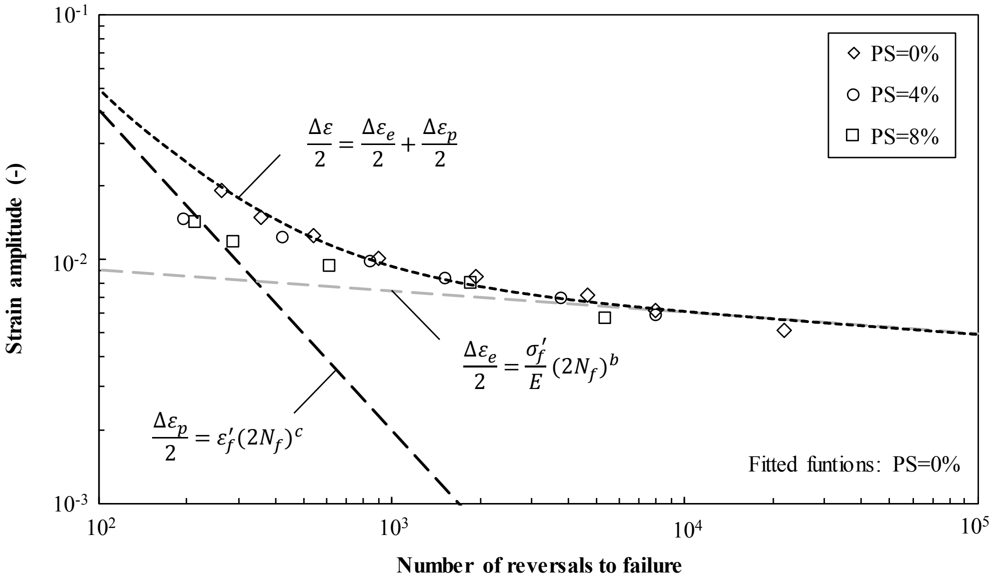

Fig. 4. Strain versus life curves of the 7050-T6 aluminium alloy at various pre-strain levels.

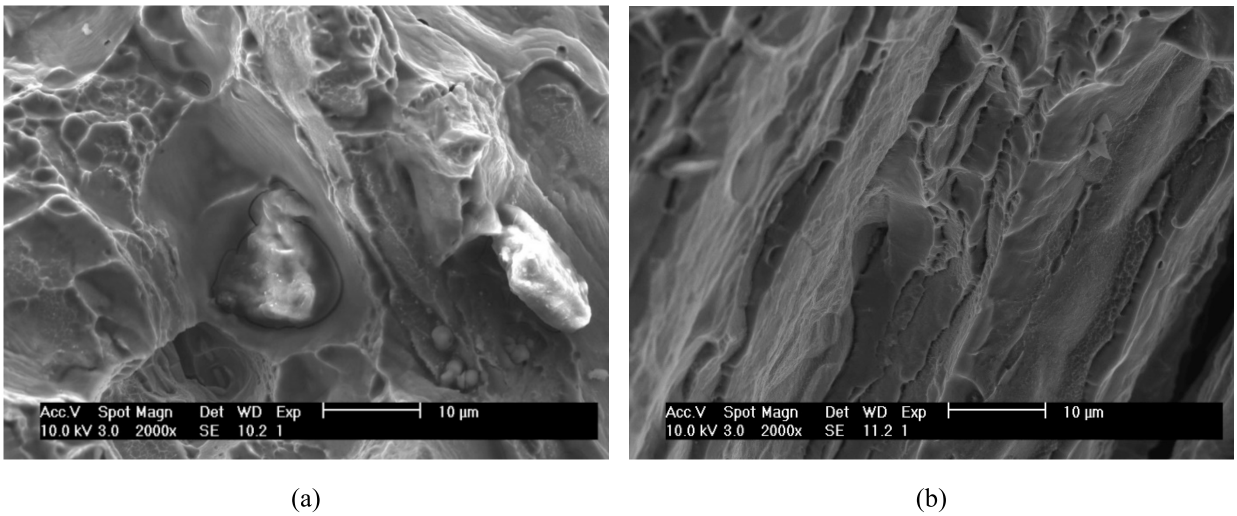

Fig. 5. Strain versus life curves of the 7050-T6 aluminium alloy at various pre-strain levels: (a) $\Delta\varepsilon/2=1.5\%$ and PS=8%; (b) $\Delta\varepsilon/2=0.6\%$ and PS=8%;

fatigue failure are clearly observed, i.e. fatigue striations, secondary cracks, cleavage planes, and ductile dimples. Overall, at lower strain amplitudes, fracture surfaces are dominated by cleavage planes and a population of secondary cracks; at higher strain amplitudes, there is a mix of cleavage facets and ductile dimples.

4. Conclusions

This study aimed at studying the effect of pre-strain on cyclic plastic behaviour of the 7050-T6 aluminium alloy. Three different series of tests were conducted under fully-reserved strain-controlled conditions with 0% pre-strain, 4% pre-strain, and 8% pre-strain. After the tests, fracture surfaces were examined by SEM. The following conclusions can be drawn:

- In the absence of pre-strain, regardless of the strain amplitude, a cyclic strain-softening behaviour was found. Cyclic stress-strain response is characterised by a short initial softening period, a dominant steady-stable stage, and final stage with rapid drop of load until failure occurs;
- The introduction of pre-strain resulted in a mixed cyclic strain softening-hardening behaviour. At higher strain amplitudes, there is a cyclic strain-softening behaviour which leads to a strain-hardening behaviour at lower strain amplitudes;
- The higher the pre-strain level, the lower is the fatigue life expectancy. The reductions tend to be more relevant at higher strain amplitudes;
- Fractography analysis reveals different mechanisms associated with the strain amplitude. At lower strain amplitudes, fracture surfaces are dominated by cleavage planes and secondary cracks, while at higher strain amplitudes, there is a mix of dimples and cleavage facets.

Acknowledgements

The authors would like to acknowledge the sponsoring under the project No. 016713 (PTDC/EMS-PRO/1356/2014) financed by Project 3599: Promover a Produção Científica e Desenvolvimento Tecnológico e a Constituição de Redes Temáticas (3599-PPCDT) and FEDER funds.

References

1. Heinz, A., Haszler, A., Keidel, C., Moldenhauer, S., 2000. Recent development in aluminium alloys for aerospace applications. Material Science & Engineering A 280, 102- 07.
2. Rometschy, P., Zhang, Y., Knight, S., 2014. Heat treatment of 7xxx series aluminium alloys - Some recent developments. Transactions of Nonferrous Metals Society of China 24, 2003-2017.
3. Branco, R., Costa, J.D., Antunes, F.V., Perdigão, S., 2016. Monotonic and cyclic behavior of DIN 34CrNiMo6 tempered alloy steel. Metals 6, 98.
4. Wang, Y., Yu, D., Chen, G., Chen, X., 2013. Effects of pre-strain on uniaxial ratcheting and fatigue failure of Z2CN18.10 austenitic stainless steel. International Journal of Fatigue 52, 106-113.
5. Borrego, L.P., Abreu, L.M., Costa, J.D., Ferreira, J.M., 2009. Analysis of low cycle fatigue in AlMgSi aluminium alloys. Engineering Failure Analysis 11, 715-725.
6. Ahmadzadeh, G.R., Varvani-Farahani, A., 2016. Fatigue damage and life evaluation of SS304 and Al 7050-T7541 alloys under various multiaxial strain paths by means of energy-based fatigue damage models. Mechanics of Materials 98, 59-70.